

## VUV-absorption cross section of CO<sub>2</sub> at high temperatures and impact on exoplanet atmospheres

Olivia Venot<sup>1,2,3,a</sup>, Nicolas Fray<sup>4</sup>, Yves Bénilan<sup>4</sup>, Marie-Claire Gazeau<sup>4</sup>, Eric Hébrard<sup>1,2</sup>, Gwenaëlle Larcher<sup>4</sup>, Martin Schwell<sup>4</sup>, Michel Dobrijevic<sup>1,2</sup>, and Franck Selsis<sup>1,2</sup>

<sup>1</sup>Univ. Bordeaux, LAB, UMR 5804, F-33270, Floirac, France

<sup>2</sup>CNRS, LAB, UMR 5804, F-33270, Floirac, France

<sup>3</sup>Instituut voor Sterrenkunde, Katholieke Universiteit Leuven, Celestijnenlaan 200D, 3001 Leuven, Belgium

<sup>4</sup>Laboratoire Interuniversitaire des Systèmes Atmosphériques, UMR CNRS 7583, Universités Paris Est Créteil (UPEC) et Paris Diderot (UPD), Créteil, France

**Abstract.** Ultraviolet (UV) absorption cross sections are an essential ingredient of photochemical atmosphere models. Exoplanet searches have unveiled a large population of short-period objects with hot atmospheres, very different from what we find in our solar system. Transiting exoplanets whose atmospheres can now be studied by transit spectroscopy receive extremely strong UV fluxes and have typical temperatures ranging from 400 to 2500 K. At these temperatures, UV photolysis cross section data are severely lacking. Our goal is to provide high-temperature absorption cross sections and their temperature dependency for important atmospheric compounds. This study is dedicated to CO<sub>2</sub>, which is observed and photodissociated in exoplanet atmospheres. We performed these measurements for the 115 - 200 nm range at 300, 410, 480, and 550 K. In the 195 - 230 nm range, we worked at seven temperatures between 465 and 800 K. We found that the absorption cross section of CO<sub>2</sub> is very sensitive to temperature, especially above 160 nm. Within the studied range of temperature, the CO<sub>2</sub> cross section can vary by more than two orders of magnitude. This, in particular, makes the absorption of CO<sub>2</sub> significant up to wavelengths as high as 230 nm, while it is negligible above 200 nm at 300 K. To investigate the influence of these new data on the photochemistry of exoplanets, we implemented the measured cross section into a 1D photochemical model. The model predicts that accounting for this temperature dependency of CO<sub>2</sub> cross section can affect the computed abundances of NH<sub>3</sub>, CO<sub>2</sub>, and CO by one order of magnitude in the atmospheres of hot Jupiter and hot Neptune.

### 1 Introduction

Exoplanets exhibit a wide variety of mass, radius, orbits, and host stars. Because of observational biases, most known transiting exoplanets are very close to their parent stars and are highly irradiated, implying large UV fluxes and high atmospheric temperatures. The atmosphere of transiting hot Jupiters and hot Neptunes can be studied by spectroscopy at the primary transit [1–6] and at the secondary eclipse [7–10]. Photochemistry has an important influence on the atmospheric composition

---

<sup>a</sup>e-mail: olivia.venot@ster.kuleuven.be

of these exoplanets, from the top of the atmosphere down to 100 mbar [11–13]. For these exoplanets and within this large pressure range, the temperature can vary roughly from 400 to 2500 K. To model correctly the photochemistry of these planets, we need to use absorption cross sections consistent with these temperatures for all the species whose photolysis plays an important role in either the formation/destruction of molecules or in the penetration of the UV flux into the atmosphere. Carbon dioxide ( $\text{CO}_2$ ) is one of these species. It has been observed in extrasolar giant planet atmospheres [7, 8], but cross section measurements ( $\sigma_{\text{CO}_2}(\lambda, T)$ ) are extremely sparse above room temperature.

The first experiments dedicated to the determination of absorption cross sections of  $\text{CO}_2$  at temperatures different from 298 K were motivated by solar system planetary studies (Mars, Titan, Venus, primitive Earth) so were performed at lower temperatures [14–17]. Some high-temperature measurements have been performed in the past but only at a few wavelengths [18, 19]. These measurements were limited to a narrow range of wavelengths and do not provide complete spectra. Nevertheless, they showed that the absorption of  $\text{CO}_2$  increases at high temperature. Spectra between 190 and 355 nm were obtained at very high temperatures (900–4500 K) by [20–22] and some of them fitted the strong temperature dependence of  $\sigma_{\text{CO}_2}(\lambda, T)$  with an empirical function.

To our best knowledge, no measurements exist of the absorption cross section of  $\text{CO}_2$  between 300 and 900 K in the wavelength range useful for exoplanetary studies (<190 nm). We resume here the results that have been published in [23], that is to say the measurements of the absorption cross section of  $\text{CO}_2$  at 300, 410, 480, 550 K between 115 and 200 nm, as well as between 195 and 230 nm at seven temperature values between 465 and 800 K. We also determine a semi-empirical formula to fit the temperature dependence for wavelengths longer than 170 nm. Finally, we study the effect of these new data on the atmospheric composition predicted by a 1D photochemical model of hot exoplanet atmospheres.

## 2 Experimental methods

We used gaseous  $\text{CO}_2$  of 99.995% purity. Tunable VUV light between 115 and 200 nm was obtained from the synchrotron radiation facility BESSY in Berlin and measurements in the 195 - 230 nm range were performed at the Laboratoire Interuniversitaire des Systèmes Atmosphériques (LISA) in Créteil, France. In both cases, an oven (Nabertherm) was used to heat the cell to a temperature of 1400 K. A figure of our experimental setup and more details about the experimental methods and the calculation of the absorption cross section are detailed in [23].

## 3 Results and discussion

### 3.1 Photoabsorption cross section from 115 nm to 200 nm

Before heating the gas, we measured ambient temperature (300 K) spectra of  $\text{CO}_2$  in order to calibrate and compare it with the previously published data [15–17]; our measurements agree very closely with these measurements with a difference of less than a few percentage points for all wavelengths. Our measurements at room temperature did not go up to 200 nm, so between 170 and 200 nm we use the data of [16].

Then, we measured  $\sigma_{\text{CO}_2}(\lambda, T)$  at three different temperatures: 410 ( $\pm 15$ ) K, 480 ( $\pm 25$ ) K, and 550 ( $\pm 30$ ) K. We show these data in Fig. 1. Between 115 and 120 nm we see a change of the cross section which depends on the temperature. At 120 nm, the absorption cross section is ten times higher at 550 K than at 300 K. Slight differences of up to 50% can be observed between 125 and

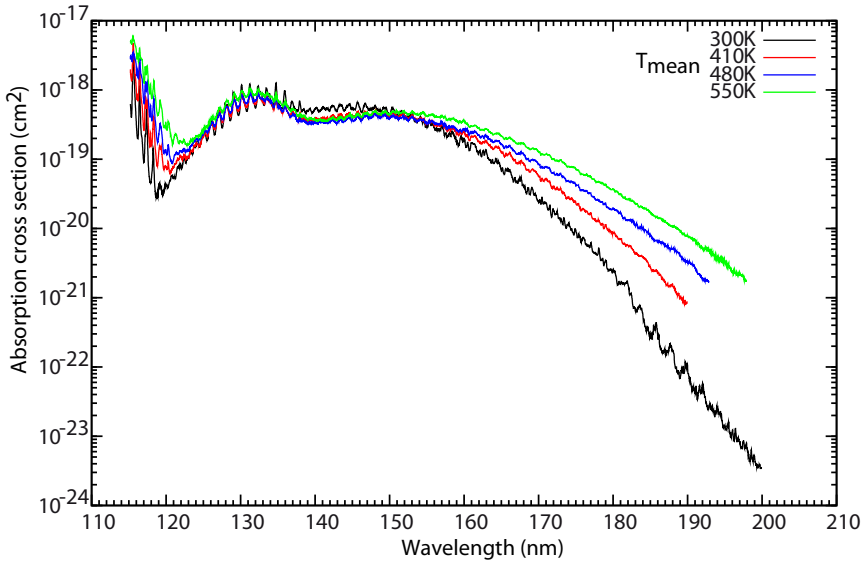


**Figure 1.** Absorption cross section of  $\text{CO}_2$  at  $T_{\text{mean}} = 300$  K (black), 410 K (red), 480 K (green) and 550 K (blue) for wavelengths between 115 and 200 nm.

140 nm while between 140 and 150 nm differences are minor. After 160 nm, we clearly observe large differences between the different temperatures. The slope of the cross section varies with the temperature. The higher the temperature is, the less steep is the slope. At 195 nm, there is a factor  $\sim 200$  between  $\sigma_{\text{CO}_2}(\lambda, 300 \text{ K})$  and  $\sigma_{\text{CO}_2}(\lambda, 550 \text{ K})$ .

### 3.2 Photoabsorption cross section from 195 nm to 230 nm

We measured  $\sigma_{\text{CO}_2}(\lambda, T)$  at seven different temperatures:  $465 (\pm 20)$  K,  $510 (\pm 25)$  K,  $560 (\pm 30)$  K,  $610 (\pm 35)$  K,  $655 (\pm 45)$  K,  $750 (\pm 55)$  K and  $800 (\pm 60)$  K. As for the cross section at shorter wavelengths, we clearly see the dependence on the temperature in this wavelength range and the increase of the cross section for high temperatures (Fig. 2). As we plotted the data obtained previously at shorter wavelengths in this figure, we see good agreement between the two ranges. Especially, we see that  $\sigma_{\text{CO}_2}(\lambda < 200 \text{ nm}, 550 \text{ K})$  matches almost perfectly with  $\sigma_{\text{CO}_2}(\lambda > 195 \text{ nm}, 560 \text{ K})$ .

### 3.3 Determination of an empirical law

For wavelengths longer than 170 nm, we parametrize the variation of  $\ln(\sigma_{\text{CO}_2}(\lambda, T) \times \frac{1}{Q_v(T)})$  with a linear regression

$$\ln\left(\sigma_{\text{CO}_2}(\lambda, T) \times \frac{1}{Q_v(T)}\right) = a(T) + b(T) \times \lambda \quad (1)$$

with  $T$  in K and  $\lambda$  in nm and where  $a(T) = -42.26 + (9593 \times 1.44/T)$ ,

$$b(T) = 4.82 \times 10^{-3} - 61.5 \times 1.44/T,$$

and

$$Q_b(T) = (1 - \exp(-667.4 \times 1.44/T))^{-2} \times (1 - \exp(-1388.2 \times 1.44/T))^{-1} \times (1 - \exp(-2449.1 \times 1.44/T))^{-1}$$

is the partition function. Figure 2 compares the absorption cross sections obtained with this calculation to the measurements. We can see that the parametrization is very good.

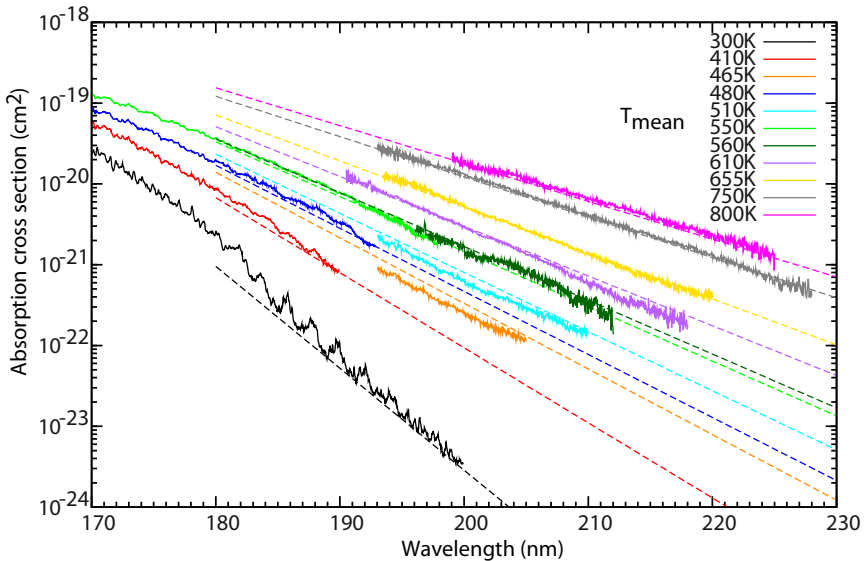


**Figure 2.** Absorption cross section of  $\text{CO}_2$  for wavelengths longer than 195 nm at 465 K, 510 K, 560 K, 610 K, 655 K, 750 K, and 800 K, plotted with the cross section at ambient temperature (black) and the absorption cross sections measured at shorter wavelengths and presented in Fig. 1 (300 K, 410 K, 480 K, and 550 K). The absorption cross sections calculated with Eq. 1 are plotted with the same color coding.

A discussion about transitions between electronic states and our parametrization can be found in [23], as well as a discussion about the disagreement between our data and the data of [21].

## 4 Application to exoplanets

We investigated the impact of the temperature dependency of the  $\text{CO}_2$  cross section on a prototype planet whose characteristics are similar to those of the hot Neptune GJ 436b [24, 25]. We chose this planet because the temperature of its upper atmosphere is around  $\sim 500$  K which corresponds to the highest temperature for which we measured the cross section between 115 and 200 nm. We considered three different types of host stars: an M, a G, and an F star. We used the spectra of GJ 644 (M3V, [26]), the Sun (G2V, [27]), and HD 128167 (F2V, [28]), scaled to get the bolometric flux received by GJ436b (Figure 9 in [23]).

We used the model described in [13] and the same temperature profile as [12] calculated by [29]. Although this is not a realistic assumption, we used the same temperature profile for all three host stars (Figure 10 in [23]). To model the vertical mixing, we considered an eddy diffusion coefficient constant  $K_{zz} = 10^8 \text{cm}^2 \cdot \text{s}^{-1}$ . Elemental abundances of the atmosphere of this planet are highly uncertain [9, 30]. So we assumed a heavy elemental enrichment of 100 compared with solar abundances [31], which is

arbitrary but higher only by a factor of 2 than the carbon enrichment of Uranus and Neptune ([32] and references therein). Consequently we obtained a high abundance of  $\text{CO}_2$ .

$\text{CO}_2$  has two routes to photodissociate :



Depending on the energy of the photons, one route is favored over the other. The quantum yield used for these two photolyses,  $q_4(\lambda)$  and  $q_5(\lambda)$ , are presented in Table 1 [33]. We assume that they remain the same at high temperature.

Quantum yield	Values [wavelength range]
$q_4(\lambda)$	1 [167-227]
$q_5(\lambda)$	variable [50-107] ; 1 [108-166]

**Table 1.** Quantum yields for the photodissociations of  $\text{CO}_2$

First, we find the steady-state composition of these atmospheres using the absorption cross sections available in the literature, which means at ambient temperature. Then, we replace the "ambient cross section" of  $\text{CO}_2$  ( $\sigma_{\text{CO}_2}(300 \text{ K})$ ) by the cross section measured at 550 K, between 115 and 200 nm ( $\sigma_{\text{CO}_2}(550 \text{ K})$ ). For wavelengths between 200 and 230 nm, we use Eq.1 to determine  $\sigma_{\text{CO}_2}(550 \text{ K})$ .

As we see in Fig. 3 (left), changing the absorption cross section of  $\text{CO}_2$  has consequences on the abundances of some species. For instance, when considering an M star, the abundance of  $\text{CO}_2$  at  $5 \times 10^{-4}$  mbar reduces by 45% when we use  $\sigma_{\text{CO}_2}(550 \text{ K})$  instead of  $\sigma_{\text{CO}_2}(300 \text{ K})$ . The compounds  $\text{O}({}^3\text{P})$ ,  $\text{CO}$ , and  $\text{NH}_3$  are also affected by the change of  $\sigma_{\text{CO}_2}(T)$ . We see that other species are also affected by the change of  $\text{CO}_2$  absorption cross section, such as  $\text{NH}_3$ ,  $\text{CH}_4$ ,  $\text{HCN}$ ,  $\text{H}_2$ , and  $\text{N}_2$ . To see these variations, we represented in Fig. 3 (right) the differences of abundances of the major species (i.e., for species with an abundance superior to  $10^{-10}$ ) between the two models. We see that the differences in abundances can reach almost  $10^5\%$ , even for species which are not directly linked to  $\sigma_{\text{CO}_2}(T)$ , such as  $\text{HCN}$  in the case of the M star.

These differences are easily comprehensible. We chose the case of  $\text{NH}_3$  to illustrate it. At high temperature, the absorption cross section of  $\text{CO}_2$  is higher around 120 nm and for wavelengths superior to 150 nm, so  $\text{CO}_2$  absorbs more UV flux than with the ambient cross section. Consequently, more  $\text{CO}_2$  is photolysed. The UV photons that are now absorbed by  $\text{CO}_2$  were absorbed by  $\text{NH}_3$  when using  $\sigma_{\text{CO}_2}(300 \text{ K})$ . Now  $\text{NH}_3$  absorbs fewer UV photons, so less is destroyed. This can be generalized to the other species. Indeed, the general behavior of these curves can be explained in terms of the various opacity sources that peak at slightly different altitudes. Because of the competition among the different opacity sources in the atmosphere, all the species absorbing in the same range of wavelength as  $\text{CO}_2$  are affected.

It is with the G star that the difference of composition is the least important when we change  $\sigma_{\text{CO}_2}$ . This is quite normal because the flux received by the planet before 200 nm is lower than with the M star and the F star (see Fig. 3). On the contrary, the difference of composition is the most important in the case F star, because it is the most important flux between 115 and 230 nm.

A discussion about the loss rates of  $\text{CO}_2$  in the different cases studied is in [23].

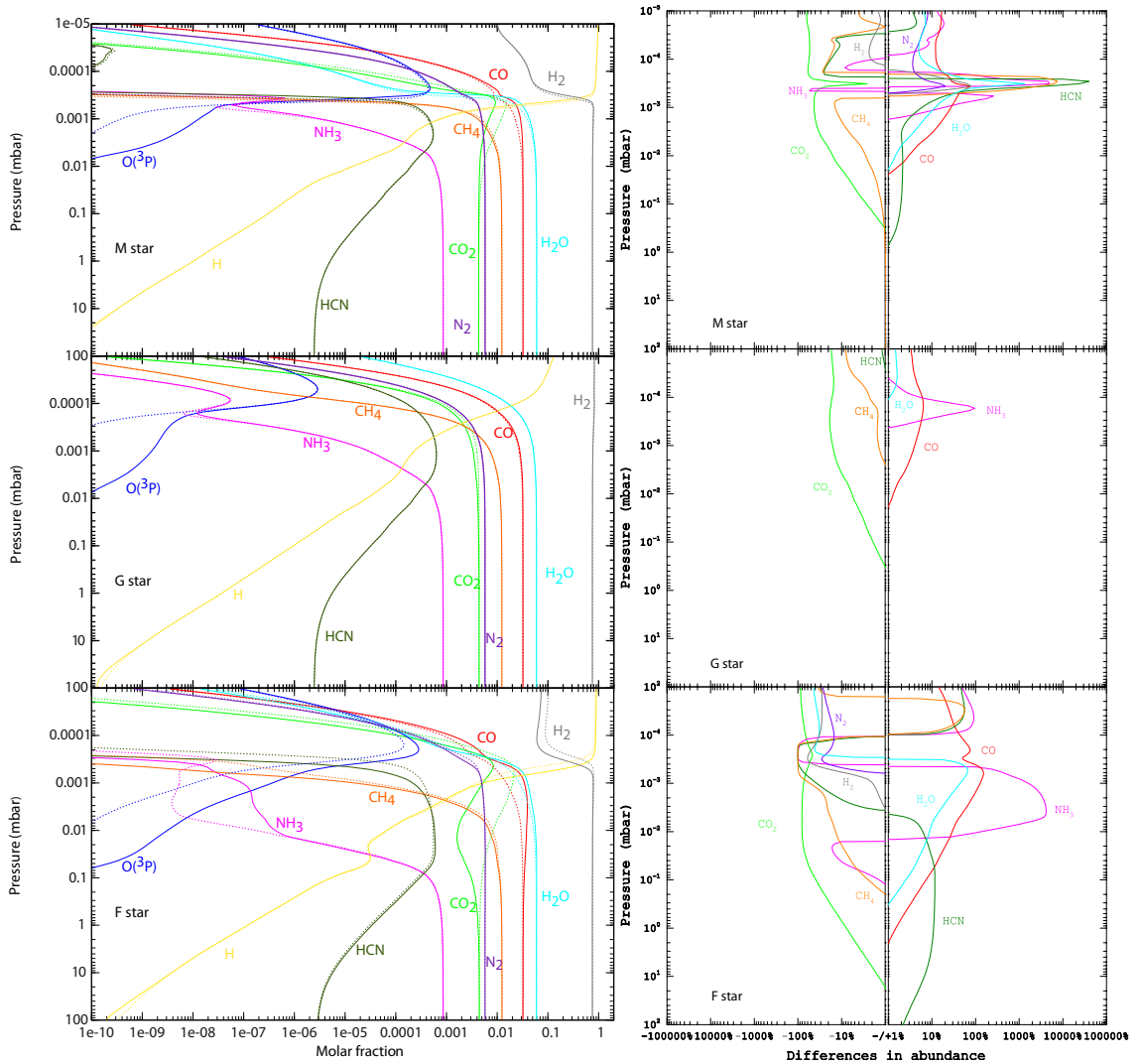


**Figure 3.** *Left:* Comparison of the atmospheric composition of GJ 436b using  $\sigma_{\text{CO}_2}(300 \text{ K})$  (dotted line) and  $\sigma_{\text{CO}_2}(550 \text{ K})$  (full line) when the planet orbits an M star (top), a G star (middle) and an F star (bottom). *Right:* Differences in abundances (in %) between the results obtained with  $\sigma_{\text{CO}_2}(300 \text{ K})$  and  $\sigma_{\text{CO}_2}(550 \text{ K})$  for species that have an abundance superior to  $10^{-10}$ , for an M star (top), a G star (middle), and an F star (bottom).

## 5 Conclusion

We measured absorption cross sections of carbon dioxide at high temperatures for the first time, in the range 115–230 nm. Between 115 and 200 nm, we measured  $\sigma_{\text{CO}_2}(\lambda, T)$  at four temperatures: 300, 410, 480, and 550 K. For longer wavelengths, we made measurements at the following temperatures: 465, 510, 560, 610, 655, 750, and 800 K. For  $\lambda > 160 \text{ nm}$ , we clearly see that the absorption cross section increases with the temperature. Thanks to the quasi-linear variation of  $\ln(\sigma_{\text{CO}_2}(\lambda, T) \times \frac{1}{Q_v(T)})$

after 170 nm, we parametrize the variation of  $\ln(\sigma_{\text{CO}_2}(\lambda, T) \times \frac{1}{Q_w(T)})$  with a linear regression which allows us to calculate  $\sigma_{\text{CO}_2}(\lambda, T)$  at any temperature in the range 170-230 nm. As we show for GJ 436b, these new data have a considerable influence on the loss rate of  $\text{CO}_2$  [23], and on the atmospheric composition of exoplanets that possess high atmospheric temperatures. Placing a hot Neptune around different stars (M, G, and F), we find that the F star is the star for which the change of absorption cross section has the most influence.

To model hot exoplanets, we recommend using cross sections relevant to the atmospheric temperature when available, or at least, as close as possible to the atmospheric temperature. Carbon dioxide is not the only absorbing species of exoplanet atmospheres. The influence of the absorption cross section of  $\text{CO}_2$  on the atmospheric composition of GJ 436b is only illustrative because the photochemistry results from the fact that species shield each other according to their abundances and their cross sections. We expect that the effect of  $\sigma_{\text{CO}_2}(\lambda, T)$  will be more important on other types of atmospheres, in particular  $\text{CO}_2$ -rich atmospheres. But the real impact of the temperature dependence of  $\sigma_{\text{CO}_2}(\lambda, T)$  can be evaluated only by taking into account the temperature dependence of all the other cross sections. Here, we simply show that it is necessary to establish this dependence for all species that absorb UV radiation. This work on  $\text{CO}_2$  is a first step towards this goal. Because [13] show that  $\text{NH}_3$  is an important absorber around 200 nm and that it absorbs UV flux very deep in the atmosphere (in pressure regions that can be probed with observations), we plan to measure the absorption cross section of this molecule at temperatures higher than 300 K. Finally, a great deal of work remains to be done in this area which is essential for the photochemical modeling of hot exoplanet atmospheres, whether terrestrial or gaseous.

## References

- [1] G. Tinetti, A. Vidal-Madjar, M. Liang, J. Beaulieu, Y. Yung, S. Carey, R. Barber, J. Tennyson, I. Ribas, N. Allard et al., *Nature* **448**, 169 (2007)
- [2] G. Tinetti, M. Liang, A. Vidal-Madjar, D. Ehrenreich, A. Lecavelier des Etangs, Y. Yung, *The Astrophysical Journal Letters* **654**, L99 (2007)
- [3] M. Swain, G. Vasisht, G. Tinetti, *Nature* **452**, 329 (2008)
- [4] J. Beaulieu, D. Kipping, V. Batista, G. Tinetti, I. Ribas, S. Carey, J. Noriega-Crespo, C. Griffith, G. Campanella, S. Dong et al., *Monthly Notices of the Royal Astronomical Society* **409**, 963 (2010)
- [5] G. Tinetti, P. Deroo, M.R. Swain, C.A. Griffith, G. Vasisht, L.R. Brown, C. Burke, P. McCullough, *The Astrophysical Journal Letters* **712**, L139 (2010)
- [6] J.P. Beaulieu, G. Tinetti, D.M. Kipping, I. Ribas, R.J. Barber, J.Y.K. Cho, I. Polichtchouk, J. Tennyson, S.N. Yurchenko, C.A. Griffith et al., *The Astrophysical Journal* **731**, 16 (2011)
- [7] M. Swain, G. Tinetti, G. Vasisht, P. Deroo, C. Griffith, J. Bouwman, P. Chen, Y. Yung, A. Burrows, L. Brown et al., *The Astrophysical Journal* **704**, 1616 (2009)
- [8] M. Swain, G. Vasisht, G. Tinetti, J. Bouwman, P. Chen, Y. Yung, D. Deming, P. Deroo, *The Astrophysical Journal Letters* **690**, L114 (2009)
- [9] K. Stevenson, J. Harrington, S. Nymeyer, N. Madhusudhan, S. Seager, W. Bowman, R. Hardy, D. Deming, E. Rauscher, N. Lust, *Nature* **464**, 1161 (2010)
- [10] K. Stevenson, J. Harrington, N. Lust, N. Lewis, G. Montagnier, J. Moses, C. Visscher, J. Blecic, R. Hardy, P. Cubillos et al., *The Astrophysical Journal* **755**, 9 (2012)
- [11] J. Moses, C. Visscher, J. Fortney, A. Showman, N. Lewis, C. Griffith, S. Klippenstein, M. Shabram, A. Friedson, M. Marley et al., *The Astrophysical Journal* **737**, 15 (2011)

- [12] M. Line, G. Vasisht, P. Chen, D. Angerhausen, Y. Yung, *The Astrophysical Journal* **738**, 32 (2011)
- [13] O. Venot, E. Hébrard, M. Agundez, M. Dobrijevic, F. Selsis, F. Hersant, R. Bounaceur, *Astronomy & Astrophysics* **546**, A43 (2012)
- [14] B. Lewis, J. Carver, *Journal of Quantitative Spectroscopy and Radiative Transfer* **30**, 297 (1983)
- [15] K. Yoshino, J.R. Esmond, Y. Sun, W.H. Parkinson, K. Ito, T. Matsui, *J. Quant. Spectrosc. Radiat. Transfer* **55**, 53 (1996)
- [16] W.H. Parkinson, J. Rufus, K. Yoshino, *Chemical Physics* **290**, 251 (2003)
- [17] G. Stark, K. Yoshino, P.L. Smith, K. Ito, *Journal of Quantitative Spectroscopy & Radiative Transfer* **103**, 67 (2007)
- [18] M. Koshi, M. Yoshimura, H. Matsui, *Chemical Physics Letters* **176**, 519 (1991)
- [19] N. Generalov, S. Losev, V. Maksimenko, *Optics and Spectroscopy* **15**, 12 (1963)
- [20] R. Jensen, R. Guettler, J. Lyman, *Chemical physics letters* **277**, 356 (1997)
- [21] C. Schulz, J. Koch, D. Davidson, J. Jeffries, R. Hanson, *Chemical Physics Letters* **355**, 82 (2002)
- [22] M. Oehlschlaeger, D. Davidson, J. Jeffries, R. Hanson, *Chemical physics letters* **399**, 490 (2004)
- [23] O. Venot, N. Fray, Y. Bénilan, M.C. Gazeau, E. Hébrard, G. Larcher, M. Schwell, M. Dobrijevic, F. Selsis, *Astronomy & Astrophysics*, accepted (2013), arXiv: 1302.2432
- [24] R. Butler, S. Vogt, G. Marcy, D. Fischer, J. Wright, G. Henry, G. Laughlin, J. Lissauer, *The Astrophysical Journal* **617**, 580 (2004)
- [25] J. Southworth, *Monthly Notices of the Royal Astronomical Society* (2010)
- [26] A. Segura, J. Kasting, V. Meadows, M. Cohen, J. Scalo, D. Crisp, R. Butler, G. Tinetti, *Astrobiology* **5**, 706 (2005)
- [27] C. Gueymard, *Solar Energy* **76**, 423 (2004)
- [28] A. Segura, K. Krelove, J. Kasting, D. Sommerlatt, V. Meadows, D. Crisp, M. Cohen, E. Mlawer, *Astrobiology* **3**, 689 (2003)
- [29] N. Lewis, A. Showman, J. Fortney, M. Marley, R. Freedman, K. Lodders, *The Astrophysical Journal* **720**, 344 (2010)
- [30] N. Madhusudhan, S. Seager, *The Astrophysical Journal* **729**, 41 (2011)
- [31] N. Grevesse, A. Sauval, *Space Science Reviews* **85**, 161 (1998)
- [32] F. Hersant, D. Gautier, J. Lunine, *Planetary and Space science* **52**, 623 (2004)
- [33] W. Huebner, J. Keady, S. Lyon, *Solar photo rates for planetary atmospheres and atmospheric pollutants* (Kluwer Academic Pub, 1992)